Fluid-Mineral Interactions: A Tribute to H. P. Eugster
© The Geochemical Society, Special Publication No. 2, 1990
Editors: R. J. Spencer and I-Ming Chou

Fe-Ti oxide-silicate equilibria: Assemblages with orthopyroxene

DONALD H. LINDSLEY
Department of Earth and Space Sciences, State University of New York, Stony Brook, New York 11794, U.S.A.

B. RONALD FROST
Department of Geology and Geophysics, University of Wyoming, Laramie, Wyoming 82071, U.S.A.

DAVID J. ANDERSEN
P.O. Box 121, Van Buren, Maine 04785, U.S.A.

and

PAULA M. DAVIDSON
Department of Geological Sciences, University of Illinois at Chicago, Chicago, Illinois 60680, U.S.A.

Abstract—In this paper equilibria are calibrated for assemblages containing orthopyroxene and two Fe-Ti oxides in the system Fe-Mg-Ti-Si-O. The isobarically univariant equilibria in the system Fe-Ti-Si-O that contain orthopyroxene (opx) are:

$$\underset{\text{quartz}}{2\,SiO_2} + \underset{\text{ulvöspinel}}{2\,Fe_2TiO_4} = \underset{\text{ilmenite}}{2\,FeTiO_3} + \underset{\text{opx}}{Fe_2Si_2O_6} \quad \text{(QUI1Op)}$$

$$\underset{\text{opx}}{Fe_2Si_2O_6} + \underset{\text{ulvöspinel}}{2\,Fe_2TiO_4} = \underset{\text{ilmenite}}{2\,FeTiO_3} + \underset{\text{fayalite}}{2\,Fe_2SiO_4} \quad \text{(OpUI1O)}$$

The important isobaric divariant equilibria in this system include: titanomagnetite-ilmenite + orthopyroxene or olivine, titanomagnetite-orthopyroxene + quartz or olivine, ilmenite-orthopyroxene + quartz or olivine.

In the QUI1Op and OpUI1O assemblages oxygen fugacity is over-determined. If the oxides retain their original composition (as in many volcanic rocks) then these assemblages can be used to obtain oxygen fugacity, temperature, pressure, and silica activity. If the oxides have re-equilibrated these equilibria can still be used to obtain oxygen fugacity, temperature, and silica activity, provided the pressure can be estimated. In a similar manner the isobaric divariant assemblages can be used to obtain two of the intensive variables: temperature, pressure, oxygen fugacity, or silica activity (if the other two variables can be estimated).

Although strictly applicable only to Ca-free orthopyroxenes, these equilibria have important applications to silicic volcanic rocks that contain low-Ca orthopyroxenes. A porphyritic obsidian from Little Glass Mountain, California, contains two oxides and orthopyroxene. Silica activity and pressure co-vary; a_{SiO2} would be 0.83 at 1 kbar and 0.63 at 6 kbar. A rhyolite from Taupo is over-determined; it contains two oxides, two pyroxenes, olivine, and quartz. All phases except augite appear to have equilibrated at 870°C and 1.6 kbar. A porphyritic rhyolitic obsidian from Inyo Craters that contains quartz, Opx, and two oxides appears to have equilibrated at 8.7 kbars, a scarcely credible pressure—but one that should be investigated further. Orthopyroxenes from the Bishop Tuff are not in Fe-Mg exchange equilibrium with the oxides. Apparent pressures range from 0.75 to *minus* 1.7 kbar. If we adjust the orthopyroxene compositions to be in Fe-Mg exchange equilibrium with the Ti-magnetite, the corresponding pressures range from 1650 to 2575 bars; values that are less scattered and considerably more plausible!

INTRODUCTION

IN A PREVIOUS PAPER (FROST *et al.*, 1988) we noted that oxygen fugacity in rocks is reflected both in the composition of the iron-titanium oxides and in the composition of the coexisting ferromagnesian silicates. We also showed how, in iron-rich systems, the equilibrium

$$\underset{\text{quartz}}{SiO_2} + \underset{\text{ulvöspinel}}{2\,Fe_2TiO_4} = \underset{\text{ilmenite}}{2\,FeTiO_3} + \underset{\text{fayalite}}{Fe_2SiO_4} \quad (1)$$

which we abbreviate as QUI1F, relates the composition of the Fe-Ti oxides to that of olivine. This equilibrium is the algebraic sum of the Fe-Ti oxide

geothermometer with the displaced FMQ equilibrium (or with the displaced metastable FHQ equilibrium). The importance of this equilibrium lies in the fact that it reduces the uncertainty inherent in the Fe-Ti oxide thermometer by an order of magnitude and it allows the petrologist to "see through" much of the re-equilibration that naturally affects Fe-Ti oxides in plutonic rocks. It is well known that fayalite + quartz are topologically equivalent to orthopyroxene, which becomes stable with increasing pressure or Mg content. In this paper we calculate oxide-silicate equilibria involving orthopyroxene, either with or without olivine or quartz, and discuss the petrologic implications of the resulting equilibria. We use the mineral abbreviations listed in Table 1. In these abbreviations we distinguish between Ca-free or Ca-poor orthopyroxene (Op, Opx) and Ca-bearing pyroxenes (P). Although the activity of $Fe_2Si_2O_6$ is defined in pigeonite and augite as well as in orthopyroxene, we have yet to wed the complex expressions that do this (DAVIDSON and LINDSLEY, 1989) with the QUI1F expressions. Thus in this paper we consider only orthopyroxene. We discuss in depth the phase equilibria of systems with orthopyroxenes and two oxides, with or without olivine or quartz. The presence of Ca in natural rocks alters the location of the pyroxene-bearing equilibria in log fO_2 – a_{SiO_2} – $\mu MgFe_{-1}$ space but does not change the topologic relations between these surfaces. Our companion papers on the Ca-bearing system will calculate the Ca-bearing equilibria and will deal more extensively with application of these equilibria to natural systems. In this paper we use the term pyroxene QUIIF in a broad sense to include equilibria involving orthopyroxene and two or more of the remaining phases Ti-magnetite, ilmenite, olivine, and quartz.

TOPOLOGIC RELATIONS

To illustrate how the topology of the Mg-bearing systems containing orthopyroxene relates to the topology of QUI1F in the iron-rich system, we first address the system Fe-Mg-Si-O (SPEIDEL and NAFZIGER, 1968), after which it will be easier to discuss the topology of the titanium-bearing system.

Table 1. Mineral abbreviations used in this paper

F = fayalite ($X_{Fa} > 0.9$)	P = pyroxene (Ca-bearing)
O = olivine ($X_{Fa} < 0.9$)	Op, Opx = orthopyroxene (little or no Ca)
H = hematite	Q = quartz
M = Ti-free magnetite	U = ulvospinel$_{ss}$ (Ti-bearing Mt)
Il = ilmenite$_{ss}$	

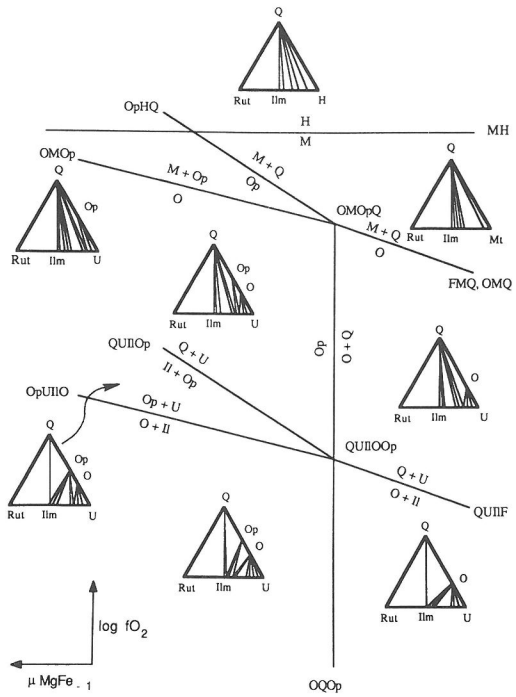

FIG. 1. Schematic isobaric, isothermal, log fO_2 – $\mu MgFe_{-1}$ diagram showing topologic relations in the system Fe-Mg-Ti-Si-O. Abbreviations as in Tables 1, 2 and 3. The upper part of the diagram refers to the Ti-free portion of the system, and the lower part to the Ti-bearing portion. The vertical OQOp curve is degenerate; none of those phases contains appreciable Ti. Thus the M-absent curve from the upper invariant point coincides with the Il-absent curve from the lower point. Compositions of phases are projected from O and Mg onto the Fe-Si-Ti plane.

System Fe-Mg-Si-O

The best way to envision this system is to consider isobaric-isothermal log fO_2-X_{Fe} sections. Because we are interested in the composition of orthopyroxene, which is not present throughout the section, we plot $\mu MgFe_{-1}$ instead of X_{Fe} as the compositional variable (Fig. 1). The numerical value of the exchange operator $\mu MgFe_{-1}$ is simply the difference $\mu_{Mg_2SiO_4}$ – $\mu_{Fe_2SiO_4}$ (or $\mu_{MgSiO_3} - \mu_{FeSiO_3}$, since these differences must be equal under conditions of exchange equilibrium) (THOMPSON *et al.*, 1982). The equilibria involved in this system are listed in Table 2. The substitution of Mg into olivine displaces the FMQ equilibrium (which becomes OMQ) to higher oxygen fugacities. At some critical value of $\mu MgFe_{-1}$, olivine + quartz is no longer stable and orthopyroxene appears instead (the OQOp equilibrium). The intersection of this reaction with the OMQ surface generates two other equilibria:

Table 2. Buffers and equilibria in the system Fe-Mg-Si-O

$2\ Fe_3O_4 + 3\ SiO_2 = 3\ Fe_2SiO_4 + O_2$	(FMQ; OMQ)
$2\ Fe_2O_3 + 2\ SiO_2 = 2\ Fe_2SiO_4 + O_2$	(FHQ; OHQ)
$2\ Fe_3O_4 + 6\ SiO_2 = 3\ Fe_2Si_2O_6 + O_2$	(OpMQ)
$2\ Fe_3O_4 + 3\ Fe_2Si_2O_6 = 6\ Fe_2SiO_4 + O_2$	(FMOp; OMOp)
$2\ Fe_2O_3 + 4\ SiO_2 = 2\ Fe_2Si_2O_6 + O_2$	(OpHQ)
$2\ Fe_2O_3 + 3\ Fe_2Si_2O_6 = 6\ Fe_2SiO_4 + O_2$	(FHOp; OHOp)
$6\ Fe_2O_3 = 4\ Fe_3O_4 + O_2$	(MH)

Plus exchange equilibria between any two pairs of Op, O, and oxides.

$$\underset{\text{magnetite}}{2\ Fe_3O_4} + \underset{\text{quartz}}{6\ SiO_2} = \underset{\text{orthopyroxene}}{3\ Fe_2Si_2O_6} + O_2 \quad \text{(OpMQ)}$$

$$\underset{\text{magnetite}}{2\ Fe_3O_4} + \underset{\text{orthopyroxene}}{3\ Fe_2Si_2O_6} = \underset{\text{olivine}}{6\ Fe_2SiO_4} + O_2 \quad \text{(OMOp).}$$

With increasing $\mu MgFe_{-1}$ both of these equilibria move to higher oxygen fugacities, the OpMQ equilibrium plotting above the OMOp equilibrium. Although it is not important to the present discussion, at very high $\mu MgFe_{-1}$ both the OpMQ and the OMOp surfaces must intersect the HM buffer. The assemblage orthopyroxene-hematite-magnetite-quartz is known from metamorphosed iron-formations (BUTLER, 1969), but the authors are not aware of any stable association of olivine with hematite, indicating that the intersection of OMO with HM lies at values of $\mu MgFe_{-1}$ that are not commonly attained in geologic environments.

System Fe-Mg-Ti-Si-O

In the Ti-bearing system the OMQ, OpMQ, and OMOp curves, which are isobarically, isothermally univariant in the Fe-Mg-Si-O system, become divariant surfaces that curve toward lower oxygen fugacities with increasing value of the $TiFe^{2+}Fe^{3+}_{-2}$ exchange vector. This occurs because Ti preferentially substitutes into the oxides relative to the silicates and into hematite relative to magnetite, lowering the ferric/ferrous ratio in the oxides. At sufficiently high values of $\mu TiFe^{2+}Fe^{3+}_{-2}$, the displaced HM equilibrium intersects the OMQ, OpMQ, and OMOp surfaces, generating the family of orthopyroxene-QUI1F equilibria: QUI1F, OpUI1O, and QUI1Op (Table 3). When discussing these pyroxene-bearing equilibria in general we refer to them as pyroxene QUI1F to emphasize the relation between them and the initial QUI1F equilibrium described by FROST *et al.* (1988).

Topologically the relation between QUI1Op and OpUI1O is similar to that between OMQ and OMOp (Fig. 1). Both equilibria move to higher oxygen fugacities with increasing $\mu MgFe_{-1}$, with QUI1Op lying above OpUILO. However, unlike the OMOp and OpMQ surfaces, the pyroxene-QUI1F surfaces cannot attain oxygen fugacities above those of the HM buffer, since they are defined by the intersection of the *displaced* HM equilibrium with the OMOp or OpMQ surfaces.

The relationship between the isobarically, isothermally univariant equilibria and the isobarically, isothermally divariant surfaces that lie between them is shown in Fig. 1 by use of chemographic projections from oxygen and magnesium onto the Si-Fe-Ti plane. In these chemographies the redox assemblages listed in Table 2 are shown as three-phase assemblages. It is important to note that each specific three-phase field shown in the chemographic triangles on Fig. 1 is valid only for a given oxygen fugacity (as well as fixed T and P); the positions of the tie lines and tie triangles shift to higher Ti in ilmenite and magnetite with decreasing oxygen fugacity. With adequate thermodynamic data, one could use any of these assemblages as a monitor of oxygen fugacity, provided the assemblage happens to be stable. The assemblage I1-U (±Q, O, or Opx) is, of course the ilmenite-magnetite oxygen barometer. The manner in which the compositions of the two Fe-Ti oxides vary as a function of T and fO_2 (at constant pressure) has been calculated by ANDERSEN and LINDSLEY (1988). How the other redox surfaces behave in isobaric, isothermal $\mu MgFe_{-1} - \mu TiFe^{2+}Fe^{3+}_{-2}$ space is presented in this paper.

In addition to acting as monitors of oxygen fugacity, some of the equilibria described above are also important indicators of silica activity. Silica activity is fixed at unity along all quartz-bearing curves (FMQ, OMQ, QUI1F, and QUI1Op). It is also buffered in any assemblage containing olivine and orthopyroxene (displaced OMOp, OpUI1O, or displaced OHOp), with a_{SiO_2} defined by the O-Op equilibria decreasing as $\mu MgFe_{-1}$ increases. Finally, silica activity and oxygen fugacity are co-variants

Table 3. QUI1F-related equilibria

$SiO_2 + 2\ Fe_2TiO_4 = 2\ FeTiO_3 + Fe_2SiO_4$	(QUI1F)
$2\ SiO_2 + 2\ Fe_2TiO_4 = 2\ FeTiO_3 + Fe_2Si_2O_6$	(QUIlOp)
$Fe_2Si_2O_6 + 2\ Fe_2TiO_4 = 2\ FeTiO_3 + 2\ Fe_2SiO_4$	(OpUIlO)

in assemblages that contain two oxides and only one ferromagnesian silicate, such as UI1O (QUI1F equilibrium displaced to $aSiO_2 < 1.0$) and UI1Op (QUI1Op equilibrium displaced to $aSiO_2 < 1.0$).

The OQOp assemblage shifts to lower values of $\mu MgFe_{-1}$ with increasing pressure and thus serves as a barometer (SPEIDEL and NAFZIGER, 1968; DAVIDSON and LINDSLEY, 1989). This pressure dependence carries over to other orthopyroxene-bearing assemblages, which can therefore provide barometric information to varying extents.

CALCULATION OF THE PYROXENE-QUI1F EQUILIBRIA

At first glance, calculation of the pyroxene-bearing QUI1F equilibria seems to be a straightforward process; it appears that all one need do is to obtain expressions for the variation of olivine and pyroxene compositions as a function of $\mu MgFe_{-1}$ and incorporate them into the QUI1F expression (FROST *et al.*, 1988). In actuality the calculations are far more complex, for at moderate to high $\mu MgFe_{-1}$, considerable Mg substitutes into the oxides as well. Furthermore, in natural systems one must also consider the presence of Ca in the pyroxenes (and even in the olivine!). As noted above, in this paper we have opted to present the Ca-free system. Ca contents up to approximately 2 mole% Wo in orthopyroxene have negligible effects, so the results presented here can also be applied to assemblages containing low-Ca orthopyroxene. (We have used the model of DAVIDSON and LINDSLEY (1989) to verify that the effect of ignoring small amounts of Ca is small. For the natural samples discussed later in the paper, we eliminated any possible errors by using activities calculated for Ca-bearing orthopyroxenes.) Orthopyroxenes having higher Wo contents may also be used, provided that the appropriate activities of Fs and En components are calculated. The sources of the solution parameters used to derive the equilibria used in this paper are shown in Table 4. Because the Fe-Mg-Ti oxide model is currently available only in thesis format (ANDERSEN, 1988), we summarize it in Appendix 1. We chose the models listed in Table 4 for reasons of consistency. For example, ANDERSEN (1988) and DAVIDSON and LINDSLEY (1989) used the same olivine model and values of parameters specifically to allow pyroxene QUIIF equilibria to be calculated. Presumably other models could be substituted, provided that standard states are made consistent; we have not done so, and thus cannot comment on possible results.

Table 4. Sources of solution parameters used to calculate orthopyroxene-QUI1F

Solution	Reference
Fe-Mg in olivine	DAVIDSON and LINDSLEY, 1989
Fe-Mg in orthopyroxene	DAVIDSON and LINDSLEY, 1989
Fe-Mg in spinels	ANDERSEN, 1988
Fe-Mg in ilmenite	ANDERSEN, 1988
Fe-Ti in ilmenite and spinel	ANDERSEN and LINDSLEY, 1988
olivine-orthopyroxene-quartz	DAVIDSON and LINDSLEY, 1989

SOURCES OF ERROR; UNCERTAINTIES IN THE RESULTS

In a system as complicated as pyroxene QUIIF, it is difficult to assess the uncertainties in the values of the calculated parameters, but they stem from three main sources: errors in the thermodynamic solution models, errors in chemical analysis of the phases, and problems with reducing analyses of complex natural minerals to the more simplified systems treated by the models. A further source of possible error is the assumption that a collection of phases in a rock represents an *equilibrium assemblage;* this is mainly the job of the petrographer. Where the pyroxene QUIIF assemblage is overdetermined, the redundant information can be used as a test of equilibrium, as illustrated in several examples in a later section.

Uncertainties introduced through the solution models cannot be treated simply, especially in the case for the Fe-Mg-Ti oxides where the parameters were extracted by the method of linear programming. That technique does not directly yield estimates of uncertainty; instead it solves for sets of parameters that are consistent with all the data *and* an arbitrarily chosen objective function. By choosing a wide range of objective functions, ANDERSEN and LINDSLEY (1988) and ANDERSEN (1988) were able to obtain the possible ranges of the model parameters, but these are *not* uncertainties in the usual sense, for the maximum value of one parameter might be possible only with, say, the minimum value of another. Fig. 3 of ANDERSEN and LINDSLEY (1988, p. 720) illustrates the ranges of temperature and oxygen fugacity allowed by the model for the Fe-Ti oxides. Within the range of experimental calibration (600–1200°C and from approximately 2 log units above to 3 units below the fO_2 of the FMQ buffer), the errors from the model itself are very small—generally less than ±10°C and ±0.1–0.2 log units for fO_2. The addition of Mg to the system (ANDERSEN, 1988) should increase these values but slightly.

As mentioned above, the models of ANDERSEN (1988) and of DAVIDSON and LINDSLEY (1989) use the same expressions for olivine, which is the common phase in the two studies. Thus errors in precision are minimized; errors in accuracy contribute ±0.1 log units in fO_2 and ±100–200 bars in calculated pressures. Errors associated with the pyroxene models are similar. Overall uncertainties resulting from the models alone are thus approximately ±10°C, ±0.2–0.3 log units in fO_2, and ±400 bars in pressure.

Typical errors associated with routine but careful microprobe analyses of oxide minerals lead to uncertainties of approximately ±0.01 in the mole fractions of the oxide components; with extreme care one can reduce the uncertainties to half that value. The larger value leads to uncertainties in temperature of ±30–100°C and in fO_2 of ±0.4–0.5 log units. Most of that range is associated with errors in the ilmenite compositions. FROST *et al.* (1988) showed how use of the QUIIF equilibrium can greatly reduce those uncertainties; the same holds for pyroxene QUIIF. It is important to note that errors become ever more important for ilmenites that contain small amounts of ferric iron (0.01 mole fraction or less), because the hematite component reflects the difference between Ti and Fe and thus is subject to the combined errors in those values. Typical errors of ±0.01 in mole fractions of pyroxene and olivine components introduce uncertainties of ±300–400 bars in pressure and ±0.1–0.2 log units in fO_2.

As to uncertainties introduced by projecting complex natural compositions to simpler compositional space, these are obviously small if the amounts of other components are small. The treatment of oxides outlined in Appendix 2 is effective for phases containing up to approximately 10% Mn components, commonly the most abundant "others". The treatment of Al is less soundly based, and one should have increasingly less confidence in the results when Al_2O_3 contents exceed 2 wt.% in Ti-magnetites. We have obtained good results for pyroxenes when the projection (LINDSLEY and AN-

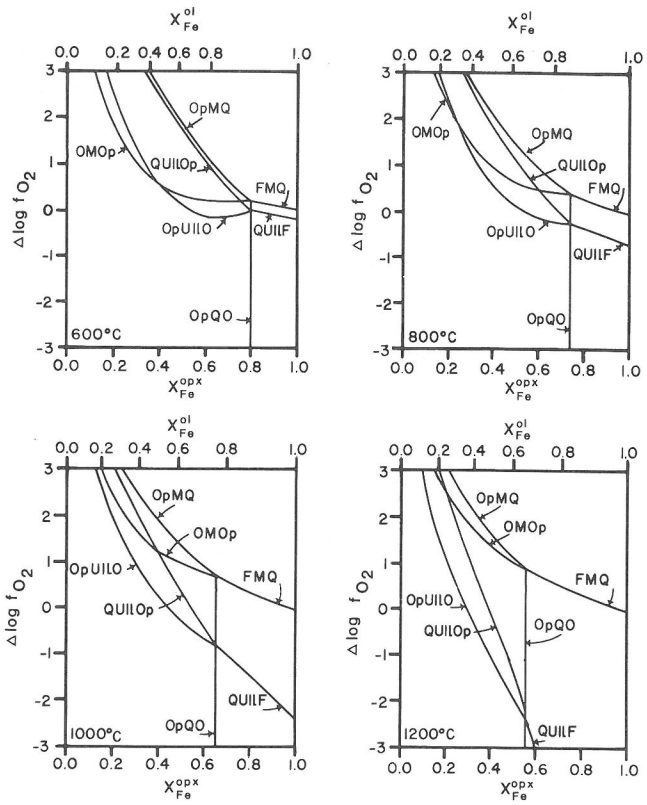

FIG. 2. $\Delta \log fO_2 - \mu MgFe_{-1}$ diagrams showing the stability of isobarically, isothermally univariant reactions in the system Fe-Mg-Ti-Si-O at 3 kilobars and 600, 800, 1000, and 1200°C. $MgFe_{-1}$ has been orthogonalized to X_{Fe}^{Opx}; $\Delta \log fO_2$ is the deviation from the FMQ buffer (= $\log fO_2 - \log fO_2$ [FMQ buffer]).

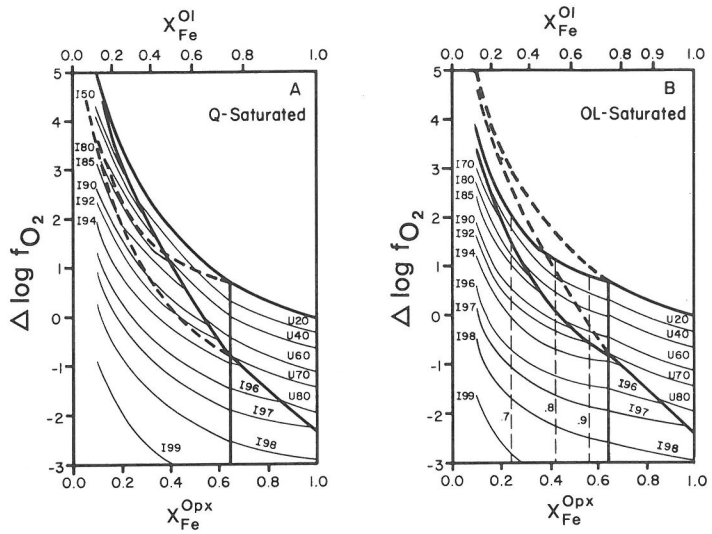

FIG. 3. $\Delta \log fO_2 - \mu MgFe_{-1}$ diagrams showing oxide compositions in some isobarically, isothermally divariant assemblages from the system Fe-Mg-Ti-Si-O at 3 kilobars and 1000°C. A = Quartz-saturated assemblages. B = Assemblages with olivine + orthopyroxene or olivine + quartz. See Fig. 1 for phases stable along univariant curves (heavy lines) and in divariant regions. Light dashed lines in B are contours for silica activity in assemblages containing olivine and orthopyroxene. Heavy dashed lines in A show metastable equilibria with olivine (see Fig. 2). Heavy dashed lines in B show metastable equilibria with quartz.

DERSEN, 1983) yields 5% or less of non-quadrilateral components. Analyses with 5–10% "others" should be viewed with caution, and those with greater than 10% should probably be used only as qualitative constraints.

APPLYING PYROXENE QUILF EQUILIBRIA

In theory, one could manipulate the expressions of the solution models to solve directly for T, P, fO_2, and a_{SiO_2}, as appropriate, for various assemblages (Table 2) and compositions. In practice, this is difficult because in the solution models, the site distributions in orthopyroxene and olivine are temperature-dependent, and thus the equations are nonlinear in temperature. [By using the Akimoto-type expression rather than the site-mixing model (ANDERSEN, 1988), we avoid that problem for the Fe-Mg-Ti spinels.] It is therefore necessary to start with an initial estimate and iterate to get the final temperature. To generate the QUI1F-related equilibria and isopleths shown in Figs. 2 through 6, we let our computer programs cycle through ranges of P, T, and compositions, as deemed appropriate from natural occurrences and experimental results. The intersections of isopleths for three-phase assemblages define points on the isobarically and isothermally univariant four-phase curves. For quartz-free orthopyroxene-olivine assemblages, we used the model of DAVIDSON and LINDSLEY (1989) to calculate values of a_{SiO_2} that were then substituted into the QUIIF equilibria to solve for fO_2.

Our pyroxene-QUIIF program is not yet user-friendly and thus not ready for distribution. It requires as input values of temperature and of pressure for all calculations, and of silica activity for all equilibria that include SiO_2. Also needed are the compositions of the oxide minerals, olivine, and orthopyroxene, as required. Then one selects the appropriate equilibria from Tables 2 and 3 and iterates through values of pressure and temperature until the various equilibria yield closely similar values for oxygen fugacity, etc. An example of the end stage of this process is given in Appendix 3.

For the reasons given by FROST *et al.* (1988), in this paper we use the variable $\Delta \log fO_2$ [defined as $\log fO_2$ (assemblage) $-$ $\log fO_2$ (FMQ buffer)] to express oxygen fugacity. Readers wishing to obtain "absolute" values of fO_2 should add back the values of FMQ as calculated from Table 1 of FROST *et al.* (1988) inasmuch as these are the terms used in calculating the oxide solution models. Note one important difference: most diagrams in FROST *et al.* (1988) use a standard state of *1 bar* and the temperature of interest. For this paper we adopt both *pressure* and temperature of interest as our standard state, a change mandated by the fact that pyroxene QUI1F reactions are more pressure-sensitive than

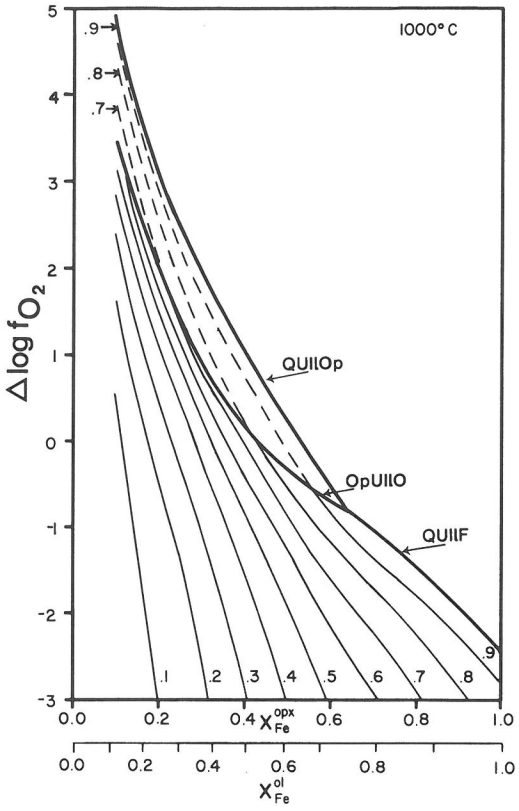

FIG. 4. $\Delta \log f_{O_2} - \mu MgFe_{-1}$ diagram contouring silica activity in assemblages with two Fe-Ti oxides at 3 kilobars and 1000°C. Dashed contours give silica activity where orthopyroxene coexists with Ti-magnetite and ilmenite; solid contours give silica activity in the assemblage olivine-Ti-magnetite-ilmenite.

those in the Mg-free system. Results from the two papers can be reconciled by adding the pressure effect on the FMQ buffer [essentially $C*(P(\text{bars}) - 1)/T(\text{K})$, where $C = 0.092$ for low quartz and 0.110 for high quartz] to the $\Delta \log f_{O_2}$ scales (FROST *et al.*, 1988).

There are so many variables in the pyroxene QUI1F expressions that it is impractical to show diagrams appropriate for all petrologically interesting conditions. Accordingly, we have chosen to illustrate some of the implications of pyroxene QUI1F using isobaric, isothermal X_{Fe} (or $\mu FeMg_{-1}$) vs $\Delta \log f_{O_2}$ diagrams (Figs. 2, 3 and 4) and isobaric $T - \Delta \log f_{O_2}$ plots (Figs. 5 and 6). Detailed discussions of the topologies of these figures are given in the ensuing pages.

Readers should especially note that the isopleths for oxides in Fig. 3 are for X_{Ti} in spinel and ilmenite. Thus for ilmenite, the isopleths show X_{FeTiO_3} *plus* X_{MgTiO_3}, which is equivalent to $(1 - X_{Fe_2O_3})$. We could have contoured both X_{FeTiO_3} and X_{MgTiO_3}, but chose to keep the diagrams as uncluttered as possible. The use of X_{Ti} is especially appropriate for the Ti-magnetites, inasmuch as the Fe-Mg-Ti spinels are reciprocal, having only three compositional variables but four possible end members (Fe_3O_4, $FeMg_2O_4$, Fe_2TiO_4, and Mg_2TiO_4). For the spinels, we define X_{Ti} as the number of Ti cations in a stoichiometric spinel having 3 cations per 4 oxygens. (We are well aware that spinels can be cation-deficient, especially at high temperatures and very low pressures. We do not consider such spinels here because the model of ANDERSEN (1988) excludes them. He did not consider nonstoichiometry, partly because pressure in many geological environments will restrict cation deficiency, but mostly because of the difficulty in analyzing spinels for vacancies. Commonly, spinels in thin-section are analyzed for Fe, Mg, Ti, Al, . . . ; then a formula based on 3 cations per 4 oxygens is calculated. The model of ANDERSEN (1988) works moderately well for experimental spinels known to be nonstoichiometric (*e.g.*, TAYLOR, 1964), when recast as 3 cations per 4 oxygens. Nevertheless, readers should be cautious in applying our methods to spinels known to have *equilibrated*—not merely to have been emplaced—at high temperatures near the Earth's surface.) Under this definition, X_{Ti} [$=Ti/(Fe^{2+} + Fe^{3+} + Mg + Ti)$] ranges from 0 to 1. By plotting X_{Ti}, we avoid possible ambiguities in assigning Ti to ulvospinel and qandelite (Mg_2TiO_4) components.

RESULTS

The calculated shapes of the pyroxene-QUI1F surfaces in $\Delta \log f_{O_2} - \mu MgFe_{-1}$ diagrams (equivalent to the topology in Fig. 1) are shown for a series of temperatures at 3 kilobars (Fig. 2). For the sake of easy visualization, the $\mu MgFe_{-1}$ axis of this figure has been orthogonalized with respect to a linear scale for X^{Opx}_{Fe}. This is not a traditional way of plotting X^{Opx}_{Fe}, for when one equates X^{Opx}_{Fe} to $\mu MgFe_{-1}$, X^{Opx}_{Fe} has a meaning even at Fe values where orthopyroxene is intrinsically unstable. A similar scale for X^{Ol}_{Fe} is also shown; this scale is nonlinear because the K_D between olivine and orthopyroxene is not unity. From these figures it is evident that the width of the orthopyroxene-magnetite-ilmenite field (bounded by the QUI1Op and OpUI1O curves) decreases markedly with increasing temperature (at constant $\Delta \log f_{O_2}$) while the intersection at which the assemblage QUI1OOp is stable migrates toward higher $\mu MgFe_{-1}$ (lower X^{Opx}_{Fe}) and lower oxygen fugacity. Decreasing pressure also tends to shrink the stability field for opx-mag-ilm, although the effect

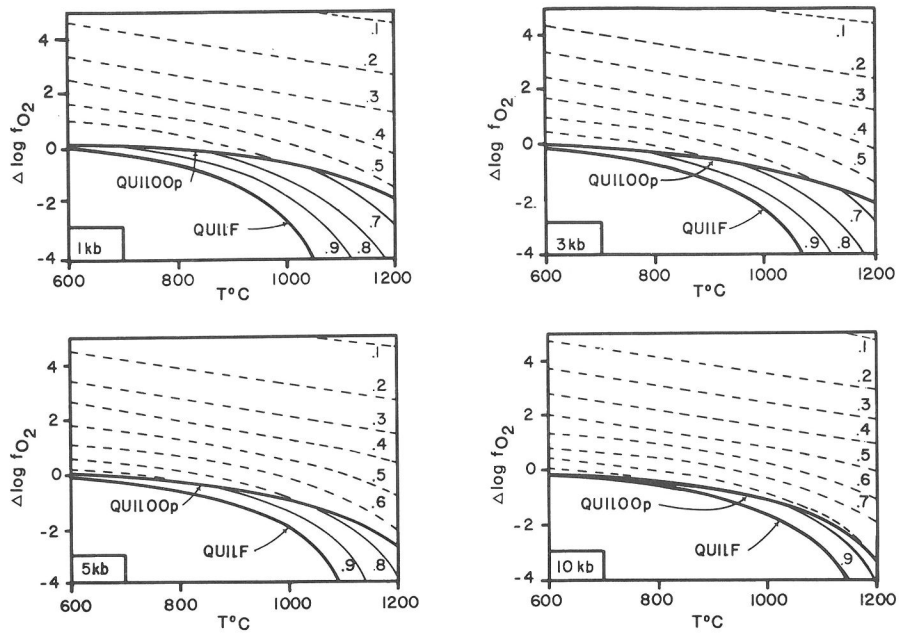

FIG. 5. Isobaric T-Δ log fO_2 diagrams showing the stability of the quartz-saturated assemblages QUI1F and QUI1Op at 1, 3, 5, and 10 kilobars. Solid contours give X_{Fe} of olivine in the QUI1F assemblage and dashed contours give X_{Fe} of orthopyroxene in the QUI1Op assemblage.

is not nearly as strong as is the effect of decreasing temperature. The major effect of decreasing pressure is to increase the stability field for olivine + quartz by driving the curve for the reaction OpQO to lower X_{Fe}.

Compositional changes of the oxides in some of the isobarically divariant assemblages can be shown by contours in the log fO_2 − μMgFe$_{-1}$ diagrams at 1000°C, with Q-saturated and OpO-saturated surfaces on separate diagrams for clarity (Figs. 3A and B). The contours mark the positions of the FMQ, OpMQ, FHQ, OpHQ, OMOp, and OHOp equilibria when the silicates are in equilibrium with the oxides whose composition are shown by the contours. The divariant assemblages OpUI1 and OUI1 are not shown in these figures because the oxide compositions in these assemblages are merely variants of the Fe-Ti oxide thermometer (ANDERSEN and LINDSLEY, 1988).

Also shown on Fig. 3B are contours for silica activity in the assemblages with olivine and orthopyroxene but lacking quartz. Since the subassemblage olivine-orthopyroxene defines silica activity, the contours for this assemblage are independent of oxygen fugacity. At a given oxygen fugacity, the assemblages orthopyroxene + two oxides and olivine + two oxides also define silica activity. The way silica activity varies in these assemblages as a function of oxygen fugacity is shown on a Δ log fO_2 − μMgFe$_{-1}$ diagram at 3 kb and 1000°C (Fig. 4).

The manner in which changes in μMgFe$_{-1}$ affect the QUI1F, QUI1Op and OpUI1O equilibria can be shown on isobaric, T − Δ log fO_2 diagrams by contouring these surfaces for the composition of olivine or orthopyroxene (Figs. 5 and 6). On these diagrams there are only two univariant curves. One is the curve for QUI1F with pure fayalite and the other is the curve for the assemblage olivine-quartz-orthopyroxene-ilmenite-magnetite (QUI1OOp). The lighter curves are contours of the QUI1F or pyroxene-QUI1F surfaces projected onto the T − Δ log fO_2 surface from T − Δ log fO_2 − μMgFe$_{-1}$ space at constant X_{Fe} in olivine or orthopyroxene. As with relations shown in Fig. 2, increasing μMgFe$_{-1}$ drives the QUI1F surface to higher fO_2 until it intersects the OQOp equilibrium. This produces the univariant assemblage QUI1OOp. With further increases in μMgFe$_{-1}$ two different QUI1F surfaces are generated: QUI1Op (Fig. 5) and OpUI1O (Fig. 6). Increasing pressure pushes the QUI1F and pyroxene-QUI1F surfaces to higher Δ log fO_2 (compare with Fig. 2). More importantly, increasing pressure also drives the QUI1OOp surface to lower oxygen fugacity such that it truncates more of the QUI1F surface. Indeed, by approximately 11–16 kbar (depending on temperature), the QUI1F surface is completely eliminated and both

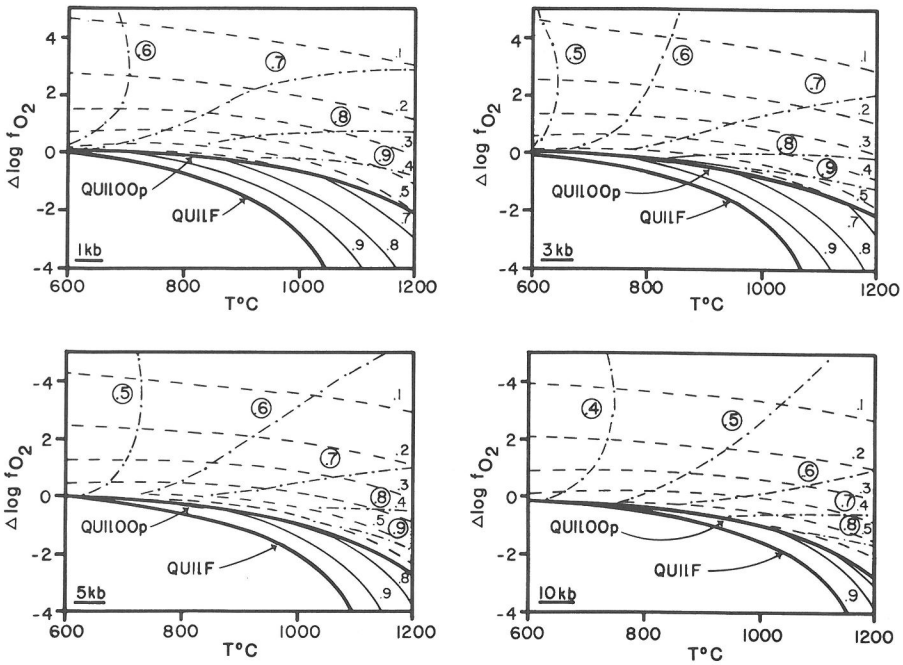

FIG. 6. Isobaric T-Δ log fO_2 diagrams showing the stability of the olivine-saturated assemblages QUI1F and OpUI1O at 1, 3, 5, and 10 kilobars. Solid contours give X_{Fe} of olivine in the QUI1F assemblage and dashed contours give X_{Fe} of orthopyroxene in the OpUI1O assemblage. Dash-dot lines are contours for silica activity in the OpUI1O assemblage. Circles values refer to isopleths for silica activity; uncircled values to isopleths of Opx or olivine composition.

the QUI1Op and the OpUI1O equilibria become stable with pure ferrosilite.

Also shown on Fig. 6 are contours for a_{SiO_2} in the assemblage OpUI1O. Of course, by definition, a_{SiO_2} for the assemblages QUI1F and QUI1OOp is unity. Accordingly, there is a strong convergence of the contours for a_{SiO_2} at low temperatures, because the slope of the OpUI1O surface in $T - \Delta \log fO_2 - \mu MgFe_{-1}$ space flattens with decreasing temperature. This flattening is so extreme that at low temperatures there are considerable portions of the OpUI1O surface, with its attendant contours of silica activity, that cannot be usefully depicted on a $T - \Delta \log fO_2$ diagram.

APPLICATIONS

The amount of information that one can obtain from assemblages (Table 5) with orthopyroxene and one or more Fe-Ti oxides is, of course, dependent on the variance of the assemblage. The assemblage olivine-orthopyroxene-quartz-ilmenite-magnetite has a phase-rule variance of two. However, the large number of equilibria among the five phases provides redundant information on the intensive variables: pressure from the silicate assemblage, and also two means of determining temperature (Fe-Ti oxide thermometer and Fe-Mg distribution in the silicates) and oxygen fugacity (Fe-Ti oxides and the position of the QUI1O or QUI1Op surface). As a result one can obtain the oxygen fugacity and temperature for this assemblage even if one or both of the oxides have re-equilibrated. Conversely, as illustrated be-

Table 5. Orthopyroxene-oxide assemblages and information they provide

Assemblage	Information
I. Assemblages in which information is over-determined (conditions can be estimated even if one phase has undergone extensive re-equilibration).	
Opx-O-Q-U-Il	P, T, fO_2
Op-Q-U-Il	P, T, fO_2
Op-O-U-Il	P, T, fO_2, a_{SiO_2}
II. Assemblages that are not over-determined	
Op-Il-U	T, fO_2, a_{SiO_2} (need P estimate)
Op-O-U	fO_2, a_{SiO_2} (need P, T estimates)
Op-O-Il	fO_2, a_{SiO_2} (need P, T estimates)
Op-Q-U	fO_2 (need P, T estimates)
Op-Q-Il	fO_2 (need P, T estimates)

low, if the oxides have not equilibrated, it may be possible to demonstrate that the entire assemblage was not simultaneously at equilibrium.

The assemblages olivine-orthopyroxene-magnetite-ilmenite and orthopyroxene-quartz-magnetite-ilmenite are of higher variance, but are still very useful, for they yield temperature, pressure, and oxygen fugacity. If both temperature and pressure are known independently, then the Fe/Mg ratio of the silicates can provide the oxygen fugacity of formation, without any chemical data from the oxides (compare Fig. 2). In addition the Fe/Mg ratio of the silicates from the assemblage olivine-orthopyroxene-magnetite-ilmenite gives the silica activity (Fig. 3).

Along with the four- and five-phase assemblages described above there is a large array of three-phase assemblages (Fig. 1 and Table 5). Those assemblages that contain two oxides can give nearly as much data as the four-phase assemblages, although one cannot "see through" any reequilibration of the oxides. The other assemblages can give oxygen fugacity and silica activity if P and T are known (although the silica activity of the quartz-bearing assemblages is not a particularly valuable piece of information!). If only P is known, then these assemblages can give one a range of oxygen fugacities and silica activities.

In the absence of comprehensive solution models for all components of the phases in the pyroxene QUI1F equilibria, it is necessary to project analyses of the phases to appropriate values of the components. For olivines, we simply normalize mole fractions of Fe_2SiO_4, Mg_2SiO_4, and Ca_2SiO_4 to 1.0. This procedure ignores Mn, which may be important in some samples. We are uncertain as to its exact effects, but we strongly advise against combining Mn with Fe as some schemes do, because to do so would inappropriately increase the calculated activity of fayalite component. We use the pyroxene projection of LINDSLEY and ANDERSEN (1983) to obtain the appropriate Wo, En, and Fs endmembers. For the oxides we form end members following LINDSLEY and SPENCER (1982), but we treat the components in a different manner. In ilmenites, we normalize $FeTiO_3$, $MgTiO_3$, and Fe_2O_3 mole fractions to 1.0. Spinels are a bit trickier because there are four (rather than three) Fe-Ti-Mg end members. We discard Mn_2TiO_4 and any $FeAl_2O_4$; we then combine Fe_2TiO_4 with Mg_2TiO_4, and twice Mg_2TiO_4 with $MgFe_2O_4$ to obtain the X_{Ti} and X_{Mg} components (X_2 and X_3 of Andersen, 1988). Details of the oxide calculations are given in Appendix 2.

To illustrate the use of pyroxene QUI1F, we apply it to several volcanic assemblages as examples. Sample Cam 49 is a porphyritic obsidian from Little Glass Mountain, Medicine Lake, California; it contains Opx ($Wo_{0.022}En_{0.553}Fs_{0.425}$), Ti-magnetite ($X_{Ti} = X_2 = 0.413$; $X_{Mg} = X_3 = 0.048$), and ilmenite ($Ilm_{0.785}Hem_{0.115}Gk_{0.100}$) but no modal olivine or quartz (CARMICHAEL, 1967). Using the BUDDINGTON and LINDSLEY (1964) curves, Carmichael inferred an oxide temperature of 880°C and log fO_2 of −12.2. Applying the model of ANDERSEN (1988), we obtain 860°C. If we knew either a_{SiO_2} or P independently, we could calculate the other from the OpMQ equilibrium, the appropriate value being that which would yield the same fO_2 as that indicated by the oxides. Lacking an independent estimate of either variable, we can calculate only the covariation of a_{SiO_2} with P (Fig. 7). Values of $\Delta \log fO_2$ are shown for the calculated points; most of the variation results from the pressure effect on the FMQ buffer. Log fO_2 varies only from −12.61 (1 kbar) to −12.56 (6 kbar).

Another example is A-10, a rhyolite from Taupo that contains quartz, olivine ($Fo_{0.135}La_{0.003}$), augite, Opx ($Wo_{0.040}En_{0.256}Fs_{0.704}$), Ti-magnetite ($X_{Ti} = X_2 = 0.594$; $X_{Ti} = X_3 = 0.021$), and ilmenite ($Ilm_{0.916}Hem_{0.056}Gk_{0.028}$) reported by EWART *et al.* (1975). This is a particularly intriguing assemblage, for it should be overdetermined. EWART *et al.* inferred 900°C and log $fO_2 = -12.95$ from the oxides; they also inferred a pressure of 4640–4955 bars from the Opx-Ol-Q assemblage. FROST *et al.* (1988) applied the QUI1F equilibrium to this sample and

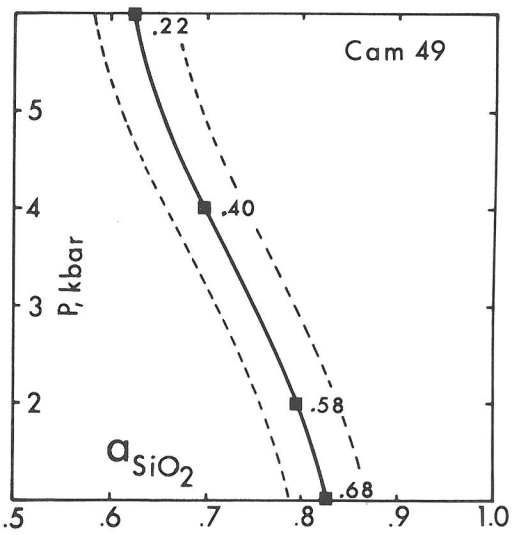

FIG. 7. Isothermal $a_{SiO_2} - P$ plot for sample Cam 49 (CARMICHAEL, 1967). Calculated points are labelled with corresponding values of $\Delta \log fO_2$. Dashed lines show variation in silica activity corresponding to uncertainties of ±1% in the compositions of the oxides.

found 870°C, with $\Delta \log fO_2 = -0.3$, and a maximum pressure of 2500 bars. This temperature cannot apply to *both* pyroxenes, for pigeonite would form from augite plus Opx at temperatures slightly above 800C (DAVIDSON and LINDSLEY, 1989, Fig. 10). Although we are not concerned here with two-pyroxene equilibria, we note in passing that the graphical thermometer of LINDSLEY (1983) gives 805 and 850°C for the augite and opx, respectively. Thus the orthopyroxene may well have been in equilibrium with the olivine, quartz, and oxides; evidently the magma did not become saturated with augite until the temperature was just below the stability of pigeonite. We obtain close agreement between oxygen fugacities indicated by the oxides ($\Delta \log fO_2 = -0.59$; $\log fO_2 = -13.62$) and by the OMQ equilibrium ($\Delta \log fO_2 = -0.58$; $\log fO_2 = -13.62$) at 870°C, the temperature indicated by the oxides, with comfortably close correspondence between the observed and calculated compositions (Table 6).

We used the model of DAVIDSON and LINDSLEY (1989) to calculate the activities of pyroxene components for comparison with the other phases in A-10, and obtained fair agreement among the compositions of olivine, augite, and Opx (with quartz) at 850°C and 1.6–1.8 kbar (Table 6). As noted above, this temperature is still too high for the augite and Opx to have coexisted without forming pigeonite. EWART *et al.* (1975, p. 10) suggested that the pyroxenes and olivine might not represent equilibrium compositions. One explanation might be admixture of a slightly different magma during eruption. However, a simpler interpretation would be that the oxides, olivine, quartz, and orthopyroxene were all in equilibrium at 850–870°C, whereas augite only joined the assemblage as the magma cooled towards 800°C.

To test our expressions for the QUI1Op equilibrium, *without* olivine, we also calculated conditions for A-10 omitting all equilibria involving olivine. The temperature and oxygen fugacity—dominated by the oxides—remain unchanged; the inferred pressure is 1.3 kbar—slightly lower but within error of that inferred using the olivine. We conclude that, for this case, the QUI1Op assemblage gives reasonable pressures, an observation that is important for the next two examples.

Cam 86, a porphyritic rhyolitic obsidian from Inyo Craters, California, contains quartz, Opx ($Wo_{0.030}En_{0.317}Fs_{0.653}$), Ti-magnetite ($X_{Ti} = X_2 = 0.420$; $X_{Mg} = X_3 = 0.074$), and ilmenite ($Ilm_{0.803}Hem_{0.150}Gk_{0.047}$) (CARMICHAEL, 1967). Carmichael reported analyses of two distinct magnetites for this sample; he inferred temperatures of 920 and 960°C with corresponding $\log fO_2$ values of −11.2 and −10.6. For simplicity we compare here only with the lower-temperature (lower-X_{Ti}) sample. Because the presence of quartz fixes silica activity, we can solve for the pressure at which the oxides, quartz, and Opx would have been in equilibrium. We plot several pyroxene QUI1F equilibria in Fig. 8. The curves intersect closely at 926 ± 10°C and 8.7 ± 0.5 kbar, the latter result being totally unexpected and perhaps implausible. (Combined uncertainties from the solution models yield a total uncertainty of ±1 kbar for this calculation. Use of the other magnetite composition changes the calculated pressure by less that 200 bars.) We note that Carmichael reported 1% each of plagioclase and alkali feldspar for this sample but gave no analyses for them. It would be most interesting to obtain analyses and to apply the two-oxide, two-feldspar barometer of STORMER and WHITNEY (1984) to compare with this surprisingly high pressure. The oxides yield $\Delta \log fO_2 = 0.29$ ($\log fO_2 = -10.93$), while for the same temperature and 8.7 kbar, the displaced OpMQ equilibrium gives $\Delta \log fO_2 = 0.28$ ($\log fO_2 = -10.92$). In our calculations, we did not fix the magnesium contents of the oxides, but rather allowed them to vary so as to remain in exchange equilibrium with the Opx. The calculated X_{Mg} ($=X_3$) of the spinel is 0.037, comfortably within the range of values reported by Carmichael, and the calculated X_{Gk} is 0.038, probably within error of the reported value. This is permissive evidence that the phases were all in equilibrium and that the high pressure may be real; we remain skeptical of it.

Our last example is for the Bishop Tuff, for which analyses of numerous opx-Q-two oxide assemblages

Table 6. Reported and calculated* compositions for sample A10 (EWART *et al.*, 1975)

	Olivine		Opx		Ti-Mt		Il		
	Fo	Fa	En	Fs	X_{Ti}	X_{Mg}	Il	Hem	Gk
Reported	0.135	0.862	0.256	0.704	0.594	0.021	0.916	0.056	0.028
Calculated*	0.144	0.849	0.246	0.719	0.594	0.029	0.916	0.059	0.025

* Compositions calculated for 870°C, 1.6 kbar using the solution models; X_{Ti} and Il were fixed in the calculations.

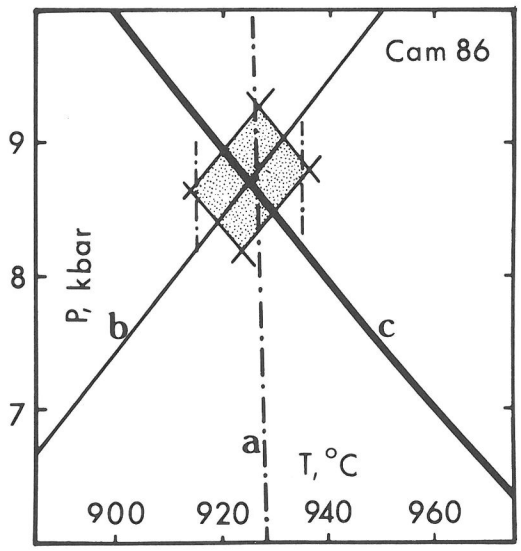

FIG. 8. *P-T* plot for sample Cam 86 (CARMICHAEL, 1967). Line **a** is for the two-oxide exchange equilibrium, which is virtually independent of pressure. Line **c** is for the displaced OpMQ equilibrium. Line **b** shows temperatures that yield the best composition for ilmenite when it is not fixed but is calculated from combined two-oxide, displaced OpMQ, and Fe-Mg exchange equilibria. The shaded area shows the effect of varying the compositions of the oxides by 1%, yielding a range in calculated temperature of 916–936°C and pressure of 8.2 to 9.3 kbar.

are available (HILDRETH, 1977). Of the 27 samples for which analyses are given, we rejected 13 because the oxides did not pass the Mg-Mn exchange test of BACON and HIRSCHMANN (1988). Of the remaining 14, we chose the seven that had the highest Mg contents reported for the oxides, because preliminary tests suggested that the oxides and Opx might not be in Fe-Mg exchange equilibrium. We first solved for the temperature and fO_2 using the oxides, and then searched for the pressure at which the OpUQ equilibrium would yield the same fO_2. The pressures ranged from 0.75 to *minus* 1.7 kbar (Fig. 9)! In all cases, the predicted Mg contents of the oxides as calculated by Fe-Mg exchange with the Opx were higher than the measured values—discrepancies that are larger than the error of the analyses. Thus we would suspect the calculated pressures even if most were not negative. As an experiment, we adjusted the compositions of the Opx until they were in Fe-Mg exchange equilibrium with the Ti-magnetites and calculated the pressures again. (Most required a decrease in X_{En} of 0.041 to 0.06; one required 0.098. These adjustments are well in excess of the probable analytical uncertainty of ±0.01.) The revised pressures (Fig. 9) range from 1.65 to 2.58 kbar, with a precision of ±0.6 kbar and an overall uncertainty of ±1.1 kbar. Thus the revised pressures show less scatter than the original values and are in good agreement with the 2–3 kbar inferred by GRUNDER *et al.* (1987) using an updated form of the two-oxide two-feldspar barometer of STORMER and WHITNEY (1985).

Unfortunately, these revised pressures are meaningless unless we assume that the Opx changed in composition by $0.041–0.098X_{En}$ *after* equilibration with the oxides and quartz. One possibility would be Fe-Mg exchange with the liquid after eruption, but the very low MgO contents of the glass (≤0.33 wt.%) would argue against that possibility. It would be interesting to analyse the glass surrounding Opx to search for gradients in MgO and FeO; such gradients would surely exist if post-eruption exchange had occurred. Any other explanation—such as incorporation of Opx "xenocrysts" upon eruption—would render the revised pressures meaningless. All we can conclude for certain at this stage is that the reported compositions of the oxides and Opx are not equilibrium values.

Thus the QUI1Op assemblage yields very reasonable pressures for the one example (Taupo A-10) for which we have an independent estimate of pressure, but bizarre results for the other two. Inyo Craters (Cam 86) appears to have been an equilibrium assemblage, but the calculated pressure is implausibly high. The Bishop Tuff examples, on the other hand, show evidence of non-equilibrium and give implausibly low pressures—but give reasonable pressures if the Opx compositions are adjusted so as to be in Fe-Mg exchange equilibrium with the Ti-magnetite. Clearly it will be necessary to test more examples before we can assess the utility of this assemblage.

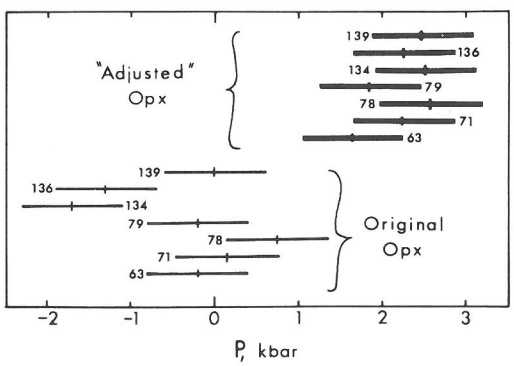

FIG. 9. Pressures inferred for seven samples of Bishop Tuff from Op-Q-U-I1 equilibria using the original compositions for Op (lower left) and compositions of Op revised so as to be in exchange equilibrium with the Ti-magnetite (upper right). Numerals are sample numbers.

CONCLUSIONS

Although this paper specifically omits Ca, therefore limiting the applicability to natural systems of the diagrams presented here, a number of useful petrologic observations can be made. One is to confirm the observation of CARMICHAEL (1967) that opx + magnetite is a relatively oxidizing assemblage, particularly if the opx is magnesian or coexists with quartz. However, the assemblage orthopyroxene-quartz-ilmenite-Ti-magnetite is not restricted to lie on a curve in $\log fO_2$-T space, as implied by CARMICHAEL (1967); rather it occupies a wide band. The exact fO_2 at which a pyroxene-bearing assemblage plots in that band is dependent on the Fe/Mg ratio of the orthopyroxene (Fig. 5). Orthopyroxene QUILF can be useful in inferring conditions of crystallization of a number of rocks, and can be especially helpful in estimating silica activities of quartz-free rocks. We plan a more complete discussion of the implications of pyroxene QUI1F in our next paper that includes the effects of Ca.

Acknowledgements—Both DHL and BRF wish to acknowledge the profound influence Hans Eugster had upon our careers, not only because Hans introduced the concept of oxygen fugacity and buffers to petrology, but also because of the personal friendships we were privileged to share with him. We have tried always to heed his exhortation: "It's all very simple: all it takes is the First and Second Law—and a little grey matter!" Research for this paper arose as part of the Laramie Anorthosite project and was funded on the following NSF grants: EAR-8416254, EAR-8618480, and EAR-8816040 (to Lindsley) and EAR-8409663, EAR-8617812, and EAR-8816604 (to Frost). Much of the solution modelling was supported by NSF grant EAR 8720185 and its predecessors. We are grateful for all this support. We also thank A. Ewart who provided us with unpublished analyses for use in this paper. We are grateful to George Fisher, Mark Ghiorso, Steve Huebner, and Richard Sack for constructive reviews that materially improved the paper.

REFERENCES

ANDERSEN D. J. (1988) Internally Consistent Solution Models for Fe-Mg-Mn-Ti Oxides. Ph.D. Dissertation, State University of New York at Stony Brook, xii + 202p.

ANDERSEN D. J. and LINDSLEY D. H. (1988) Internally consistent solution models for Fe-Mg-Mn-Ti oxides: Fe-Ti oxides. *Amer. Mineral.* **73,** 714–726.

BACON C. R. and HIRSCHMANN M. M. (1988) Mg/Mn partitioning as a test for equilibrium between coexisting Fe-Ti oxides. *Amer. Mineral.* **73,** 57–61.

BUDDINGTON A. F. and LINDSLEY D. H. (1964) Iron-titanium oxide minerals and synthetic equivalents. *J. Petrol.* **5,** 310–357.

BUTLER P. JR. (1969) Mineral compositions and equilibrium in the metamorphosed iron formation the Gagnon Region, Quebec, Canada. *J. Petrol.* **10,** 56–101.

CARMICHAEL I. S. E. (1967) The iron-titanium oxides of salic volcanic rocks and their associated ferromagnesian silicates. *Contrib. Mineral. Petrol.* **14,** 36–64.

DAVIDSON P. M. and LINDSLEY D. H. (1989) Thermodynamic analysis of pyroxene-olivine-quartz equilibria in the system CaO-MgO-FeO-SiO_2. *Amer. Mineral.* **74,** 18–30.

EWART A., HILDRETH W. and CARMICHAEL I. S. E. (1975) Quaternary acid magmas in New Zealand. *Contrib. Mineral. Petrol.* **51,** 1–27.

FROST B. R., LINDSLEY D. H. and ANDERSEN D. J. (1988) Fe-Ti oxide-silicate equilibria: Assemblages with fayalitic olivine. *Amer. Mineral.* **73,** 727–740.

GRUNDER A. L., HADJIGEORGIOU C. H., LINDSLEY D. H. and ANDERSEN D. J. (1987) Two-oxide, two-feldspar barometry revisited: I. Effect of revised calibrations (abstr.) *Geol. Soc. Amer. Abstr. Prog.* **19,** 686.

HILDRETH W. (1977) The magma chamber of the Bishop Tuff: Gradients in pressure, temperature, and composition. Ph.D. Dissertation, University of California, 328p.

LINDSLEY D. H. (1983) Pyroxene thermometry. *Amer. Mineral.* **68,** 477–493.

LINDSLEY D. H. and ANDERSEN D. J. (1983) A two-pyroxene thermometer. *J. Geophys. Res. Suppl.* **88,** A887–A906.

LINDSLEY D. H. and SPENCER K. J. (1982) Fe-Ti oxide geothermometry: Reducing analyses of coexisting Ti-magnetite (Mt) and ilmenite (Ilm). *EOS* **63,** 471.

SACK R. O. (1982) Spinels as petrogenetic indicators: activity-composition relations at low pressures. *Contrib. Mineral. Petrol.* **79,** 169–186.

SPEIDEL D. H. and NAFZIGER R. H. (1968) P-T-fO_2 relations in the system Fe-O-MgO-SiO_2. *Amer. J. Sci.* **266,** 361–379.

STORMER J. C. and WHITNEY J. A. (1984) Two-feldspar and iron-titanium oxide equilibria in silicic magmas and the depth of origin of large volume ash-flow tuffs. *Amer. Mineral.* **70,** 52–64.

TAYLOR R. W. (1964) Phase equilibria in the system FeO-Fe_2O_3-TiO_2 at 1300°C. *Amer. Mineral.* **49,** 1016–1030.

THOMPSON J. B. JR., LAIRD J. and THOMPSON A. B. (1982) Reactions in amphibolite, greenschist and blueschist. *J. Petrol.* **23,** 1–27.

APPENDIX 1: SUMMARY OF MODEL FOR Fe-Mg-Ti OXIDES

We briefly outline here the thermodynamic treatment of Fe-Mg-Ti oxides (ANDERSEN, 1988), which builds on that of SACK (1982) and ANDERSEN and LINDSLEY (1988). G_{excess} is modelled as an asymmetric Margules solution

$$G_{excess} = \sum_i \sum_{j,j\neq i} W_{ij} X_i X_j \left(X_j + \frac{1}{2} \sum_{k,k\neq i,j} X_k \right) + \sum_i \sum_{j,j\neq i} \sum_{k,k\neq i,j} W_{ijk} X_i X_j X_k. \quad \text{(A1-1)}$$

Expressions for the activity coefficients derived from Equation (A1-1) are then

$$\alpha RT \ln(\gamma_n) = \sum_i \sum_{j,j\neq i} W_{ij}(X_iX_j(X_j - X_i + 1) - \sum_{m,m\neq n} X_m(Q_j(2X_j - X_i + 1) + Q_i(X_j - 2X_i + 1))) + \sum_i \sum_{j,j\neq i} \sum_{k,k\neq i,j} W_{ijk}(X_iX_jX_k - \sum_{m,m\neq n} X_m(Q_iX_jX_k + Q_jX_iX_k + Q_kX_iX_j)) \quad \text{(A1-2)}$$

where Q_i is a term related to $\partial X_i/\partial X_m$ and $Q_i = 1$ ($m = i$), -1 ($i = n$), 0 ($m \neq i$, $i \neq n$). The temperature and pressure dependencies of the W terms are defined as

$$W = W_H - TW_S + (P - 1)W_V.$$

For ilmenite, the configurational entropy is expressed as

$$S_{conf} = -R(X_{il} \ln(X_{il}(X_{il} + X_{gk})) + X_{gk} \ln(X_{gk}(X_{il} + X_{gk})) + 2X_{hem} \ln(X_{hem})).$$

Activity expressions for il_{ss} are then

$$RT \ln(a_{il}) = RT \ln(X_{il}(X_{il} + X_{gk})) + RT \ln(\gamma_{il})$$

$$RT \ln(a_{gk}) = RT \ln(X_{gk}(X_{il} + X_{gk})) + RT \ln(\gamma_{gk})$$

$$RT \ln(a_{hem}) = RT \ln(X^2_{hem}) + RT \ln(\gamma_{hem})$$

where $RT \ln(\gamma_n)$ is derived from Equation (A1-2).

ANDERSEN (1988) used two different expressions for spinel thermodynamics; we use the simpler modified Akimoto-type model.

Because the composition of a spinel in the system Fe^{2+}-Fe^{3+}-Mg-Ti can be defined in terms of only two variables (or three components), the choice of the compositional terms is somewhat arbitrary. If N_{Ti} and N_{Mg} are taken as the independent variables, then the compositional variables can be defined as

$$X_2 = N_{Ti}$$

$$X_3 = N_{Mg}.$$

The remaining compositional variables are then

$$N_{Fe^{2+}} = 1 + N_{Ti} - N_{Mg}$$

and

$$N_{Fe^{3+}} = 2 - 2N_{Ti},$$

where the sum of the cations is given by

$$N_{Fe^{2+}} + N_{Fe^{3+}} + N_{Mg} + N_{Ti} = 3.$$

Configurational entropy for spinel is expressed as

$$S_{conf} = -R(X_2(1 + X_2 - X_3)/(1 + X_2) \ln(X_2(1 + X_2 - X_3)/(1 + X_2)) + (1 - X_2) \ln(1 - X_2) + X_2X_3/(1 + X_2) \ln(X_2X_3/(1 + X_2)) + (1 + X_2 - X_3)/(1 + X_2) \ln((1 + X_2 - X_3)/(1 + X_2)) + (1 - X_2) \ln((1 - X_2)) + X_3/(1 + X_2) \ln(X_3/(1 + X_2)) + X_2 \ln(X_2) - 2 \ln(2))$$

and the nonconfigurational energy G^* as

$$G^* = G^*_{Fe_3O_4}(1 - X_2 - X_3) + G^*_{Fe_2TiO_4}X_2 + G^*_{MgFe_2O_4}X_3 - \Delta\mu^*_{23}X_2X_3 - \frac{1}{2}\Delta\mu^*_{2q}X_2X_3(1 + X_2 - X_3) + W_{12}X_2(1 - X_2)(X_2 - X_3) + W_{21}X_2(1 - X_2) \times (1 - X_2 + X_3) + W_{13}X_3(1 + X_2 - X_3) \times (X_3 - X_2) + W_{31}X_3(1 + X_2 - X_3)(1 - X_3) + \Delta W_{q3}X_2X_3(X_2 - 1).$$

This yields three end-member energies ($G^*_{Fe_3O_4}$, $G^*_{Fe_2TiO_4}$, and $G^*_{MgFe_2O_4}$), and one reciprocal term, $\Delta\mu^*_{23}$, which is the energy difference for the reciprocal exchange

$$Fe_3O_4 + \frac{1}{2}Mg_2TiO_4 = MgFe_2O_4 + \frac{1}{2}Fe_2TiO_4$$

or

$$\Delta\mu^*_{23} = \frac{1}{2}(G^*_{Fe_2TiO_4} - G^*_{Mg_2TiO_4}) + G^*_{MgFe_2O_4} - G^*_{Fe_3O_4}.$$

The term, $\Delta\mu^*_{2q}$, is a Bragg-Williams type ordering term for mixing of $(Mg, Fe)_2TiO_4$ spinels,

$$(Fe^{2+})[Fe^{2+}Ti]O_4 + (Mg)[MgTi]O_4 = (Fe^{2+})[MgTi]O_4 + (Mg)[Fe^{2+}Ti]O_4$$

or

$$\Delta\mu^*_{2q} = (G^*_{Fe_2TiO_4} + G^*_{Mg_2TiO_4}) - (G^*_{(Fe^{2+})[MgTi]O_4} + G^*_{(Mg)[Fe^{2+}Ti]O_4}).$$

The four possible binaries would yield eight asymmetric binary coefficients, of which only five are independent since there are only ten terms in the expansion of G^*. We have chosen to define G^* in terms of the binaries Fe_3O_4-Fe_2TiO_4 (W_{12} and W_{21}), Fe_3O_4-$MgFe_2O_4$ (W_{13} and W_{31}) and $MgFe_2O_4$-Mg_2TiO_4 (ΔW_{q3}) where

$$\Delta W_{q3} = W_{q3} - W_{3q}$$

and then

$$W_{3q} = \Delta\mu^*_{23} - 2\Delta W_{q3} + 2W_{21} - W_{12}$$

$$W_{q3} = \Delta\mu^*_{23} - \Delta W_{q3} + 2W_{21} - W_{12}.$$

The subscripts for the W terms are: 1 = mt, 2 = usp, 3 = magnesioferrite, and q = Mg_2TiO_4 (qandelite).

This leads to the activity expressions:

$$RT \ln(a_{Fe_3O_4}) = \ln((1 + X_2 - X_3)(1 - X_2)^2/(1 + X_2)) + \frac{1}{2}\Delta\mu^*_{2q}X_2X_3(1 + 2X_2 - 2X_3) + \Delta\mu^*_{23}X_2X_3 + W_{12}X_2X_3 - X_2)(1 - 2X_2) + W_{21}X_2(2X_2(1 - X_2 + X_3(2X_2 - 1)) + W_{13}X_3(2X_3 - 2X_2 - 1)(X_3 - X_2) + W_{31}X_3(2X_3(1 + X_2 - X_3) - X_2) + \Delta W_{q3}X_2X_3(1 - 2X_2)$$

$$RT \ln (a_{Fe_2TiO_4}) = 2 \ln (X_2(1 + X_2 - X_3)/(1 + X_2)) + \frac{1}{2} \Delta\mu^*_{2q} X_3((X_3 - X_2)(1 - 2X_2) - 1)$$
$$+ \Delta\mu^*_{23} X_3(X_2 - 1) + W_{12}(1 - X_2)(2X_2(1 - X_2 + X_3) - X_3) + W_{21}(1 - 2X_2)(1 - X_2)$$
$$\times (1 - X_2 + X_3) + W_{13} X_3((1 + 2(X_3 - X_2))(X_3 - X_2) - 1$$
$$+ W_{31} X_3(1 + (X_3 - X_2)(1 - 2X_3)) + \Delta W_{q3} X_3(1 - 2X_2)(X_2 - 1)$$

$$RT \ln (a_{MgFe_2O_4}) = \ln (X_3(1 - X_2)^2/(1 + X_2)) + \frac{1}{2} \Delta\mu^*_{2q} X_2(1 + X_2 - X_3)(2X_3 - 1) + \Delta\mu^*_{23} X_2(X_3 - 1)$$
$$+ W_{12} X_2((X_2 - X_3)(2X_2 - 1) + X_2 - 1) + W_{21} X_2((1 + 2X_2)(1 - X_2)$$
$$+ X_3(2X_2 - 1)) + W_{13}(1 + X_2 - X_3)(2X_3(1 + X_2 - X_3) - X_2)$$
$$+ W_{31}(1 + X_2 - X_3)(2X_3 - 1)(X_3 - 1) + \Delta W_{q3} X_2(X_3(1 - 2X_2) + X_2 - 1)$$

$$RT \ln (a_{Mg_2TiO_4}) = 2 \ln (X_2 X_3/(1 + X_2)) + \Delta\mu^*_{2q}(1 + X_2 - X_3)(X_2(X_3 - 1) - \frac{1}{2} X_3)$$
$$+ \Delta\mu^*_{23}(X_2 - 1)(X_3 - 2) + W_{12}(X_2 - 1)(2X_2(X_2 - X_3) + X_3)$$
$$+ W_{21}(1 - X_2)(1 + (X_3 - X_2)(1 - 2X_2)) + W_{13}(1 + X_2 - X_3)(2(1 - X_3)(X_3 - X_2)$$
$$+ X_3) + W_{31}(1 + X_2 - X_3)(X_3 - 2)(2X_3 - 1) + \Delta W_{q3}(1 - X_2)(2X_2(X_3 - 1) - X_3).$$

Table A1-1 gives the values of the solution parameters we use.

Table A1-1. Model parameters for Fe-Mg-Ti oxides

Parameter	Preferred value	Minimum value	Maximum value
Exchange equilibria			
ΔH_{OLIL}	−1.4661527E+04	−1.4723021E+04	−1.4483356E+04
ΔS_{OLIL}	1.5187286E+01	1.5147428E+01	1.5309038E+01
ΔV_{OLIL}	−9.7300000E−02		
ΔH_{FETI}	2.9435301E+04		
ΔS_{FETI}	4.5123501E+00		
ΔH_{MGFE}	−2.8368547E+04	−2.9919742E+04	−2.7179059E+04
ΔS_{MGFE}	−1.3222971E+01	−1.4203763E+01	−1.2489809E+01
Ilmenite			
$W_{H,ig}$	8.4055215E+03	8.3486436E+03	8.4621592E+03
$W_{S,ig}$	3.0423203E+00	2.9888186E+00	3.0766625E+00
$W_{V,ig}$	1.0800000E−02		
$W_{H,gi}$	7.3635693E+03	7.3621216E+03	7.6529805E+03
$W_{S,gi}$	3.4959583E+00	3.4948959E+00	3.6954560E+00
$W_{V,gi}$	1.0800000E−02		
W_{gh}	2.6651402E+04	2.6608336E+04	2.7090381E+04
W_{hg}	2.6651402E+04	2.6608336E+04	2.7090381E+04
$W_{H,ih}$	4.4204801E+04		
$W_{S,ih}$	1.2274390E+01		
$W_{H,hi}$	1.2634250E+05		
$W_{S,hi}$	1.0060010E+02		
Spinel (Akimoto distribution)			
$\Delta\mu^*_{H,23}$	2.2323242E+04	1.6138391E+04	2.8282242E+04
$\Delta\mu^*_{S,23}$	1.3994102E+01	9.7778091E+00	1.7738436E+01
$\Delta\mu^*_{2q}$	0.0000000E+00		
W_{12}	1.5748030E+04		
$W_{H,21}$	4.6175480E+04		
$W_{S,21}$	2.3076500E+01		
W_{13}	0.0000000E+00		
W_{31}	0.0000000E+00		
$\Delta W_{H,q3}$	3.9471707E+04	3.9471707E+04	4.8350406E+04
$\Delta W_{S,q3}$	2.3178127E+01	2.3178127E+01	3.1921598E+01

```
use feti, femgilsp
tk=1043; p=2200; x2=0.2573; x3=0.034; xhem=0.105?; xgk=0.044?;
tk=1048; p=2200; x2=0.2573; x3=0.034; xhem=0.105?; xgk=0.044?;
tk=1053; p=2200; x2=0.2573; x3=0.034; xhem=0.105?; xgk=0.044?;

use domq, femgilsp, femgopxil
tk=1043; p=2200; x2=0.2573; x3=0.034?; xhem=0.105?; xgk=0.044?; xopx=0.446; yopx=0.021; aqtz=1.0;
tk=1048; p=2200; x2=0.2573; x3=0.034?; xhem=0.105?; xgk=0.044?; xopx=0.446; yopx=0.021; aqtz=1.0;
tk=1053; p=2200; x2=0.2573; x3=0.034?; xhem=0.105?; xgk=0.044?; xopx=0.446; yopx=0.021; aqtz=1.0;

use feti, femgilsp, femgopxil
tk=1043; p=2200; x2=0.2573; x3=0.034?; xhem=0.105?; xgk=0.044?; xopx=0.446; yopx=0.021; aqtz=1.0;
tk=1048; p=2200; x2=0.2573; x3=0.034?; xhem=0.105?; xgk=0.044?; xopx=0.446; yopx=0.021; aqtz=1.0;
tk=1053; p=2200; x2=0.2573; x3=0.034?; xhem=0.105?; xgk=0.044?; xopx=0.446; yopx=0.021; aqtz=1.0;

use feti, domq, femgilsp, femgopxil
tk=1043; p=2200; x2=0.2573; x3=0.034?; xhem=0.105?; xgk=0.044?; xopx=0.446?; yopx=0.021; aqtz=1.0;
tk=1048; p=2200; x2=0.2573; x3=0.034?; xhem=0.105?; xgk=0.044?; xopx=0.446?; yopx=0.021; aqtz=1.0;
tk=1053; p=2200; x2=0.2573; x3=0.034?; xhem=0.105?; xgk=0.044?; xopx=0.446?; yopx=0.021; aqtz=1.0;
```

tk	p	fo2	dfmq	ti	mg	xmg	xil	xgk	xhem	xmg
1043.0	2200.0	-14.128	0.922	0.2573	0.0340	0.0270	0.8395	0.0571	0.1034	0.0637
1048.0	2200.0	-13.960	0.977	0.2573	0.0340	0.0270	0.8360	0.0567	0.1073	0.0635
1053.0	2200.0	-13.794	1.030	0.2573	0.0340	0.0270	0.8323	0.0563	0.1114	0.0633

tk	p	fo2	dfmq	ti	mg	xmg	xil	xgk	xhem	xmg
1043.0	2200.0	-14.128	0.922	0.2573	0.0340	0.0270	0.8395	0.0571	0.1034	0.0637
1048.0	2200.0	-13.960	0.977	0.2573	0.0340	0.0270	0.8360	0.0567	0.1073	0.0635
1053.0	2200.0	-13.794	1.030	0.2573	0.0340	0.0270	0.8323	0.0563	0.1114	0.0633

tk	p	fo2	dfmq	ti	mg	xmg	xil	xgk	xhem	xmg	xopx	yopx	aqtz
1043.0	2200.0	-14.073	0.977	0.2573	0.0334	0.0265	0.8388	0.0560	0.1052	0.0626	0.4460	0.0210	1.0000
1048.0	2200.0	-13.966	0.970	0.2573	0.0339	0.0270	0.8364	0.0565	0.1071	0.0633	0.4460	0.0210	1.0000
1053.0	2200.0	-13.861	0.963	0.2573	0.0345	0.0274	0.8339	0.0571	0.1090	0.0641	0.4460	0.0210	1.0000

tk	p	fo2	dfmq	ti	mg	xmg	xil	xgk	xhem	xmg	xopx	yopx	aqtz
1043.0	2200.0	-14.129	0.921	0.2573	0.0334	0.0265	0.8407	0.0560	0.1033	0.0624	0.4460	0.0210	1.0000
1048.0	2200.0	-13.960	0.976	0.2573	0.0339	0.0270	0.8362	0.0565	0.1073	0.0633	0.4460	0.0210	1.0000
1053.0	2200.0	-13.793	1.031	0.2573	0.0345	0.0274	0.8314	0.0571	0.1115	0.0642	0.4460	0.0210	1.0000

tk	p	fo2	dfmq	ti	mg	xmg	xil	xgk	xhem	xmg	xopx	yopx	aqtz
1043.0	2200.0	-14.132	0.918	0.2573	0.0318	0.0253	0.8438	0.0532	0.1030	0.0593	0.4354	0.0210	1.0000
1048.0	2200.0	-13.960	0.977	0.2573	0.0341	0.0271	0.8358	0.0568	0.1073	0.0637	0.4471	0.0210	1.0000
1053.0	2200.0	-13.790	1.034	0.2573	0.0365	0.0290	0.8276	0.0605	0.1119	0.0682	0.4585	0.0210	1.0000

FIG. A3-1. Example of a pyroxene QUIIF calculation. The upper portion is input to the program; the lower portion is the results. The temperature 1048 K provides the best calculated composition of the ilmenite; the guess of 2200 bars provides a moderately good agreement between fO_2 from the oxides and that from the OpUQ equilibrium. 2250 bars (not shown) provided the best agreement, and was adopted is the pressure. The abbreviations are defined in the text. "?" in the input means that the preceeding value is allowed to vary during the calculations.

APPENDIX 2: CALCULATION OF OXIDE COMPONENTS

In the recalculation schemes described below, we follow the procedure of LINDSLEY and SPENCER (1982) until the last steps. We assume that the analyses have been made by electron microprobe, with no independent determination of Fe^{3+}. Even in those cases where Fe^{3+} has been determined independently, it is preferable to combine ferrous and ferric iron at the beginning. The procedure:

1. Convert analyses to atomic proportions. Convert sufficient Fe to Fe^{3+} to yield 3 cations per 4 oxygens (spinel) or 2 cations per 3 oxygens (ilmenite).

2. Form and discard Mn_2TiO_4 (spinel) or $MnTiO_3$ (ilmenite). Ignore Si if it is likely that it represents contamination from silicates. Otherwise form and discard Fe_2SiO_4 or $FeSiO_3$ if you believe the Si is actually in the oxide minerals.

3. For spinels, form $MgAl_2O_4$ and either Mg_2TiO_4 or $FeAl_2O_3$ to use up all Mg and Al. For ilmenites, assign Al to Al_2O_3 and discard; form $MgTiO_3$.

4. For spinels, form Fe_2TiO_4. The remaining Fe should be in the ratio of 1 Fe^{2+} to 2 Fe^{3+}; combine to form Fe_3O_4. For ilmenites, form $FeTiO_3$ and Fe_2O_3.

5. For spinels, normallize $MgAl_2O_4$, Mg_2TiO_4, Fe_2TiO_4, and Fe_3O_4 to 1.0. Use the normallized values to obtain $X_1 = Fe_3O_4$; $X_{Ti} = X_2 = Mg_2TiO_4 + Fe_2TiO_4$; $X_{Mg} = X_3 = 2\,Mg_2TiO_4 + MgAl_2O_4$. For ilmenites, normallize $MgTiO_3$, $FeTiO_3$, and Fe_2O_3 to 1.0, and use the normallized components.

APPENDIX 3: AN EXAMPLE OF PYROXENE-QUI1F CALCULATIONS

We illustrate our calculation methodology with an example; the data are for Bishop Tuff sample 136 (HILDRETH, 1977), with the Opx composition adjusted as discussed in the text. The upper part of Fig. A3-1 shows the input to the program. Each set of data is headed by a "use" statement of the equilibria that are to be calculated. "feti" refers to the two-oxide equilibria: the FeTi-Fe^{3+}_2 exchange and the oxidation reaction 4 Fe_3O_4 + O_2 = 6 Fe_2O_3; "domq" is the OpMQ equilibrium (Table 2) displaced by ulvospinel component in the spinel; and "femgilsp" and "femgopxil" are FeMg exchange between ilmenite and spinel and Opx and ilmenite respectively. "tk" and "p" are the trial values of temperature in kelvins and pressure in bars; "x2" and "x3" are X_{Ti} and X_{Mg} in the spinel; "xhem" and "xgk" are Fe_2O_3 and $MgTiO_3$ components of ilmenite; "xopx" and "yopx" are X_{En} and X_{Wo} in Opx. All Fe components are calculated by difference. The silica activity ("aqtz") is 1.0 because quartz is present. If there were olivine rather than quartz, the values of "aqtz" would be silica activities calculated from the programs of DAVIDSON and LINDSLEY (1989). A "?" following a number means that the value is allowed to vary in the calculation; there must be one "?" for each equilibrium that is "use"d. Thus in the first set (following "use feti, femgilsp"), the spinel is fixed and the ilmenite composition is allowed to vary so as to satisfy all three equilibria. The first three lines of numbers in the bottom part of the table are the calculated results for this set. The Fe_2O_3 content of the ilmenite is best matched at 1048 K; the calculated geikielite content is marginally high but probably within analytical error. Thus we accept 1048 K and $\log fO_2 = -13.96$ as the best values based on the oxides.

The remaining three sets of input "use" different subsets of pyroxene QUIIF equilibria; the best answer is found when all three give similar values for $\log fO_2$ *and* calculate the correct compositions. Note, for example, that x3 ($=X_{Mg}$ in spinel) is allowed to vary, but for 1048 K the calculated values (0.0339; 0.0341) are very close to the measured value (0.0340). This example is the penultimate of a number of attempts using various pressures; pressures lower than 2200 bars yield values of $\log fO_2$ for "domq" that are lower than those for "feti"; pressures greater than 2250 have the opposite effect, while the final trial value 2250 bars produced the best agreement and is accepted as the best answer. The method is tedious but effective.